nature neuroscience

Conditional dendritic spike propagation following distal synaptic activation of hippocampal CA1 pyramidal neurons

Tim Jarsky[1,4], Alex Roxin[2–4], William L Kath[1,2] & Nelson Spruston[1]

The perforant-path projection to the hippocampus forms synapses in the apical tuft of CA1 pyramidal neurons. We used computer modeling to examine the function of these distal synaptic inputs, which led to three predictions that we confirmed in experiments using rat hippocampal slices. First, activation of CA1 neurons by the perforant path is limited, a result of the long distance between these inputs and the soma. Second, activation of CA1 neurons by the perforant path depends on the generation of dendritic spikes. Third, the forward propagation of these spikes is unreliable, but can be facilitated by modest activation of Schaffer-collateral synapses in the upper apical dendrites. This 'gating' of dendritic spike propagation may be an important activation mode of CA1 pyramidal neurons, and its modulation by neurotransmitters or long-term, activity-dependent plasticity may be an important feature of dendritic integration during mnemonic processing in the hippocampus.

Excitatory synapses on distal dendrites are common in the nervous system. For example, cortical pyramidal neurons receive cortico-cortical inputs in layer 1, often hundreds of microns from the soma. Mitral cells of the olfactory bulb receive input from olfactory receptor neurons on a tuft of apical dendrites, similarly far from the soma. Purkinje cells of the cerebellum receive inputs from mossy cells, many of which terminate on distal dendrites. Synapses like these are intriguing, because their long distance from the spike initiation zone, thought to reside in the axon[1], suggests that special mechanisms may be required for these synapses to trigger action potentials.

One possible mechanism to preserve the efficacy of distal synapses is through the generation of local dendritic spikes. Indeed, all dendrites studied to date express numerous voltage-gated channels[2], and substantial evidence now supports the notion that spikes can be initiated in dendrites[3]. Unlike axonal action potentials, however, dendritic spikes do not propagate reliably over long distances in dendrites. A remaining challenge, therefore, is to determine what types of synaptic inputs can trigger dendritic spikes and how the spikes propagate along dendrites of various morphologies expressing unique combinations of channels. For such questions, a computational approach can place the available data in an integrated, quantitative framework and provide testable predictions concerning the function of various types of synapses and dendrites.

In the hippocampus, CA1 pyramidal neurons receive two distinct excitatory synaptic inputs[4]: the perforant path (or temporo-ammonic path) provides direct input from layer 3 of entorhinal cortex to the apical dendritic tuft, and the Schaffer collaterals provide input from CA3 pyramidal neurons to basal and apical dendrites in CA1. Although all of the Schaffer-collateral synapses are closer to the soma than are the perforant-path synapses, some of the Schaffer-collateral synapses are nevertheless hundreds of microns from the soma. The perforant-path projection to CA1 terminates in excitatory, glutamatergic synapses[5,6], but it is controversial whether these synapses can depolarize the somatic membrane to action-potential threshold[7–9]. Distal perforant-path and Schaffer-collateral synapses elicit dendritic spikes, both *in vitro* and *in vivo*[10,11], but some of these dendritic spikes do not propagate reliably to the soma, raising questions about the function of dendritic spikes and the conditions necessary for them to reach the soma and trigger an action potential in the axon[10–13].

Here we explored these questions by examining the impact of distal perforant-path and Schaffer-collateral synaptic inputs to CA1 pyramidal neurons, using a combined computational and experimental approach. We found that strong perforant-path activation resulted in dendritic spikes that could fail to propagate to the soma. Modest activation of Schaffer-collateral synapses in the upper apical dendrites, however, facilitated the forward propagation of tuft dendritic spikes, thus allowing action-potential output in the axon following distal synaptic activation.

RESULTS

Modeling distal synaptic activation in excitable CA1 dendrites

To assess the ability of perforant-path synapses to activate CA1 pyramidal neurons, we used compartmental models of two reconstructed neurons. Each neuron included four active conductances: a voltage-gated Na^+ conductance (G_{Na}), a delayed rectifier K^+ conductance (G_{Kdr})

[1]Institute for Neuroscience, Department of Neurobiology and Physiology, Northwestern University, 2205 Tech Drive, Evanston, Illinois 60208, USA. [2]Department of Engineering Science and Applied Mathematics, Northwestern University, 2145 Sheridan Road, Evanston, Illinois 60208, USA. [3]Unité Mixte de Recherche 8119, Centre Nationale de la Recherche Scientifique, Neurophysics and Physiology, Université René Descartes, 45 Rue des Saints Pères, 75270 Paris Cedex 06, France. [4]These authors contributed equally to this work. Correspondence should be addressed to N.S. (spruston@northwestern.edu).

Received 31 August; accepted 20 October; published online 20 November 2005; doi:10.1038/nn1599

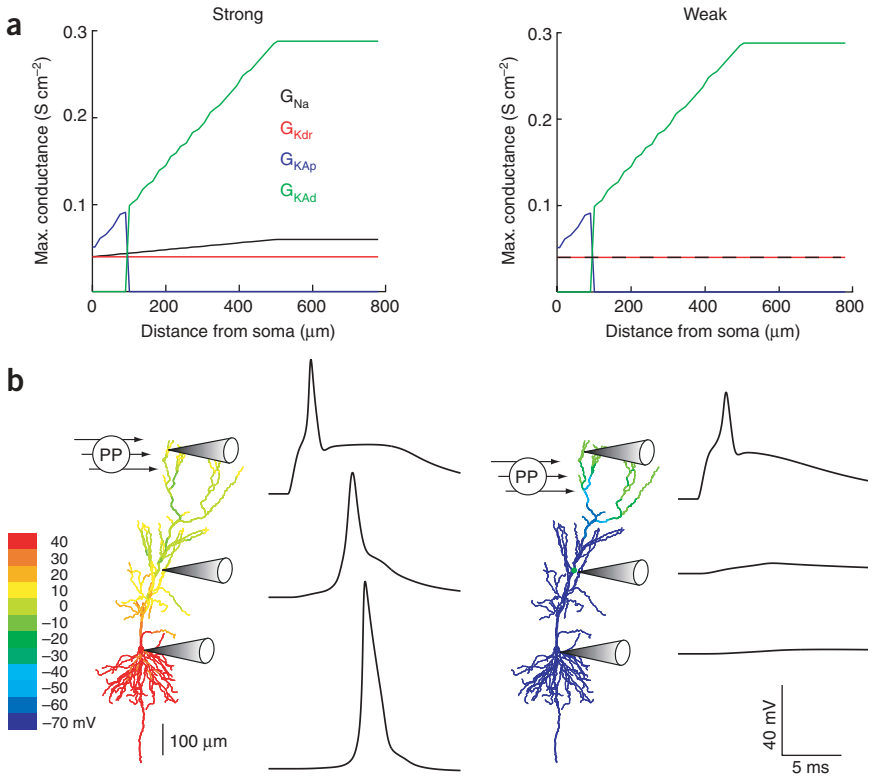

Figure 1 Strong and weak dendritic excitability models of CA1 pyramidal neurons respond differently to perforant-path activation. (**a**) Channel distributions as a function of distance from the soma in the two models. G_{Na}, voltage-gated Na^+ conductance; G_{Kdr}, delayed rectifier K^+ conductance; G_{KAp}, proximal A-type K^+ conductance; G_{KAd}, distal A-type K^+ conductance. (**b**) Perforant-path (PP) activation (10% of available synapses) triggered dendritic spikes in the apical tuft. These spikes propagate to the soma and trigger an action potential in neurons with strong (left), but not weak (right), dendritic excitability. Scales apply to both panels. Color maps are of maximal (peak) voltage in each compartment of the model. Traces are voltage versus time plots at the three dendritic locations indicated by the electrodes. Animations of these simulations in this cell and another reconstructed cell are provided in **Supplementary Videos 1–3** and **6**.

and two A-type K^+ conductances (G_{KA}). Consistent with experimental reports, G_{Na} and G_{Kdr} were modeled with moderate conductance along the somato-dendritic axis, but a higher G_{Na} in the axon made this the preferential site of action-potential initiation[14]. G_{KA} was modeled with the reported sixfold increase in conductance along the somato-dendritic axis and lower half-inactivation voltage in proximal (G_{KAp}) versus distal (GK_{Ad}) dendrites[15,16]. We used two versions of the model: a weak dendritic excitability model with uniform G_{Na} in the soma and dendrites, and a strong dendritic excitability model with a slight gradient of increasing G_{Na} with distance from the soma (**Fig. 1a**). These two models are simple compared to the full repertoire of voltage-gated channels known to be expressed in pyramidal cells[2,17]; nevertheless, these models reproduce two populations of CA1 neurons with distinct profiles of action-potential backpropagation[14]. We used these models to make experimentally testable predictions about the ability of perforant-path inputs to activate CA1 neurons.

The two models exhibited markedly different behavior (**Fig. 1**). In the strong dendritic excitability model, simulation of a strong perforant-path stimulus (10% of available synapses in the distal apical tuft) triggered the initiation of a dendritic spike, which propagated to the soma and triggered an action potential (**Fig. 1b**, left and **Supplementary Video 1** online). Similar behavior was observed in the model of a second reconstructed neuron (**Supplementary Fig. 1** online and **Supplementary Video 2** online). In the weak dendritic excitability model, the same strong perforant-path input triggered a dendritic spike, but the spike failed to propagate to the soma, thus resulting in a subthreshold somatic depolarization (**Fig. 1b**, right and **Supplementary Video 3** online). With a high-frequency burst of synaptic inputs (5 at 100 Hz), dendritic spikes sometimes propagated to the soma, but successful propagation required activating a large number of synapses (for example, 30% success at 15% of perforant-path synapses; data not shown). These results suggest that the only way perforant-path inputs can trigger an action potential in the axon is if a dendritic spike is initiated in the tuft and propagates down the apical dendrite. In the weak excitability model, forward propagation was unreliable and did not ensure an action-potential output. This finding is consistent with our previous experimental observation that dendritic spikes can occur in the absence of somatic action potentials[10,18].

Interaction between perforant-path and Schaffer-collateral inputs

In the models, when dendritic spikes failed to propagate from the distal apical tuft to the soma, they usually failed in the upper apical dendrite (**Fig. 1b**, right; **Supplementary Figs. 2** and **3** online; **Supplementary Videos 3–8** online). We therefore investigated how perforant-path synaptic responses were influenced by the activation of synapses in the upper apical dendrites, just below the apical tuft. These synapses correspond to distal Schaffer-collateral inputs. When perforant-path and Schaffer-collateral inputs are activated together, action-potential firing is probabilistic, depending on the exact number and location of the randomly selected synapses activated in each region. Action-potential probability was determined from more than 170,000 simulations and plotted as a function of the percentage of perforant-path and Schaffer-collateral synapses activated (**Fig. 2**).

In the strong dendritic excitability model, two modes of activation were apparent. In the first mode of the strong excitability model (**Fig. 2b**, left, region 1), activation of the Schaffer collaterals (>3%) was on its own sufficient to trigger action potentials on at least some trials. With little or no activation of perforant path, action-potential probability increased from 0 to 1 over a narrow range of Schaffer-collateral activation (about 3–5%). As the percentage of perforant-path inputs was increased from 0% to 2%, the percentage of Schaffer-collateral inputs necessary to trigger an action potential 50% of the time (green in **Fig. 2b**, left) decreased from about 4% to 3%. In this mode, the Schaffer-collateral input was stronger than the perforant-path input and dendritic spikes almost always began in the upper apical dendrites, below the tuft and near the Schaffer-collateral inputs (green in **Fig. 2c**, left, region 1).

In the second mode of the strong excitability model (**Fig. 2b**, left, region 2), perforant path was the dominant input, and action potentials could be elicited on at least some trials with >2% of the synapses activated. With little or no activation of the Schaffer collaterals, action-potential probability increased from 0 to 1 over a narrow range of

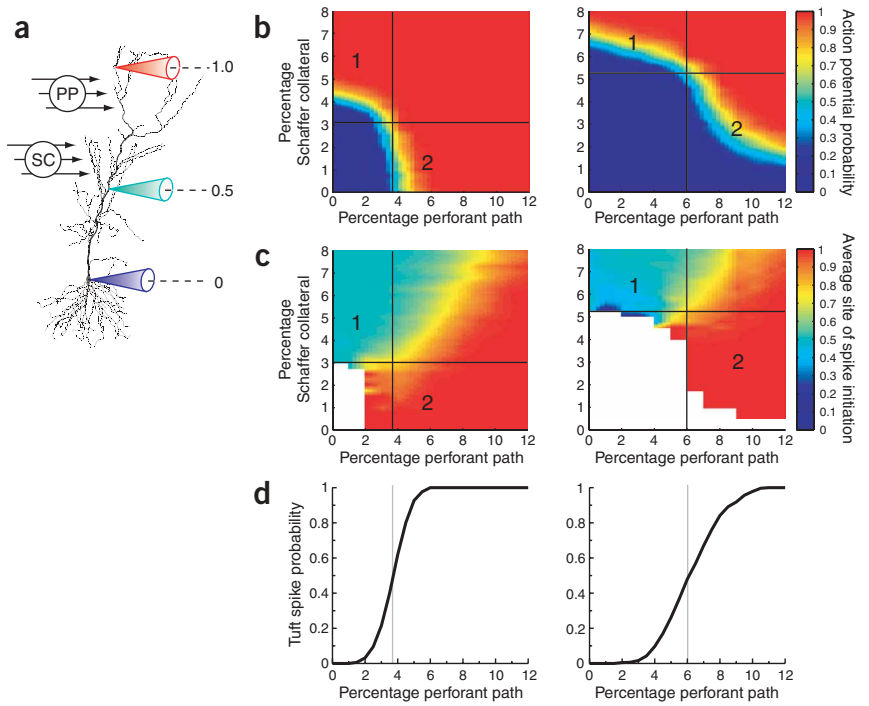

Figure 2 Modes of activation of CA1 pyramidal neurons by perforant-path and Schaffer-collateral activation. (**a**) Schematic of model cell with perforant-path (PP) and Schaffer-collateral (SC) activation sites indicated. Electrodes at indicated locations were used to determine whether spikes began in the soma (value 0, blue), mid apical dendrite (value 0.5, green) or apical tuft (value 1.0, red). (**b**) Probability of action-potential initiation (in the axon) in response to activation of different percentages of available PP (apical tuft) and SC synapses (upper apical dendrites). (**c**) Locations of spike initiation as described in **a**. Intermediate colors are determined by the fractions of trials yielding initiation at one or another site. In both **b** and **c**, regions 1 and 2 correspond to modes of activation where SC and PP inputs dominate, respectively (see text for details). (**d**) Probability of a dendritic spike in the apical tuft as a function of the percentage of PP synapses activated (no SC activation). Columns in **b**, **c** and **d** correspond to the strong and weak dendritic excitability models, respectively. Probabilities were determined from 200 trials of randomly placed synapses for each %PP, %SC pair. In **b** and **c**, horizontal guide lines correspond to the minimal percentage of SC inputs necessary to trigger an action potential; in **b**, **c** and **d**, vertical guide lines correspond to the percentage of PP inputs necessary to trigger a spike in the apical tuft on 50% of trials.

perforant-path activation (about 2–6%). In this mode, action potentials were driven by dendritic spikes originating in the apical tuft (red in **Fig. 2c**, left, region 2). With perforant-path stimulation alone, the probability of dendritic spike initiation in the tuft increased from near 0 to 1 over the same range (about 2–6%, **Fig. 2d**, left). Over this range of perforant-path activation, modest activation of the Schaffer collaterals (0–3%) reduced the percentage of perforant-path inputs necessary to trigger a propagating dendritic spike, but the spikes almost always began in the apical tuft (innervated by perforant path) and propagated to the soma (**Fig. 2c**, left). Stronger activation of either or both pathways led to reliable dendritic spike initiation, with the spikes tending to begin near the strongest synaptic input. In summary, in the strong excitability model, each input was able to trigger dendritic spikes on its own, and each input could cooperate with the other to trigger a propagating dendritic spike.

The behavior of the weak dendritic excitability model was dramatically different (**Fig. 2b**, right). Importantly, a single coincident activation of perforant-path synapses was almost never able to produce an action potential on its own. Only when perforant-path activation was increased to very high levels (>50% of all synapses) did an action potential occur in the soma (data not shown). Even then, action potentials only occurred on some trials (about 10% at 60–70% perforant-path activation), and even greater activation of perforant-path inputs decreased the probability of action-potential firing (owing to the activation of K^+ channels and the inactivation of Na^+ channels by large excitatory post synaptic potentials (EPSPs)). Because such large activation of perforant path is required, interaction of perforant-path and Schaffer-collateral inputs is a more plausible explanation for how perforant path influences action-potential firing in CA1 pyramidal neurons with weakly excitable dendrites.

In the weak dendritic excitability model, perforant-path and Schaffer-collateral inputs interacted in two important ways. First, low levels of perforant-path activation slightly reduced the percentage of Schaffer-collateral inputs necessary to trigger an action potential (**Fig. 2b**, right, region 1). Activation of between 0% and 6% of perforant-path synapses reduced the percentage of Schaffer-collateral synapses necessary to trigger an action potential 50% of the time (green in **Fig. 2b**, right) from about 6.5% to 5.2% (slope = 0.22). In this mode, most of the spikes began in the apical dendrite (below the tuft) and propagated to the soma (green in **Fig. 2c**, right, region 1), but in some cases, the Schaffer-collateral and perforant-path inputs summed in the soma to trigger an action potential first in the axon (blue in **Fig. 2c**, right, region 1). Within this activation mode, there was little difference between perforant-path inputs that triggered dendritic spikes and those that did not. Even when perforant-path activation triggered a dendritic spike (for example, 20% of the time at 5% activation: **Fig. 2d**, right), the spikes did not spread into the upper apical dendrites, below the tuft. Instead, the main effect in this mode of activation was that perforant-path inputs reduced the amount of Schaffer-collateral input necessary to trigger a dendritic spike in the apical dendrites below the tuft.

By contrast, stronger activation of perforant path (above about 6%) activated dendritic spikes in the tuft more frequently. These spikes tended to be larger and thus spread throughout the apical tuft. In this mode (**Fig. 2b**, right, region 2), activation of between 6% and 10% of perforant-path synapses reduced the percentage of Schaffer-collateral synapses necessary to trigger an action potential 50% of the time from about 5.2% to 2% (slope = 0.80). Furthermore, in this mode, action potentials almost always began as dendritic spikes in the apical tuft (red in **Fig. 2c**, right, region 2). This activation mode thus revealed an especially interesting interaction between perforant path and Schaffer collaterals. Dendritic spikes were triggered by strong perforant-path input, but their propagation to the soma was gated by Schaffer-collateral inputs. In the absence of Schaffer-collateral inputs, the apical tuft dendritic spikes failed to reach the soma and did not produce an action potential. However, even modest levels of Schaffer-collateral input were able to facilitate the forward propagation of these dendritic spikes, such that they could trigger a full action potential in the axon

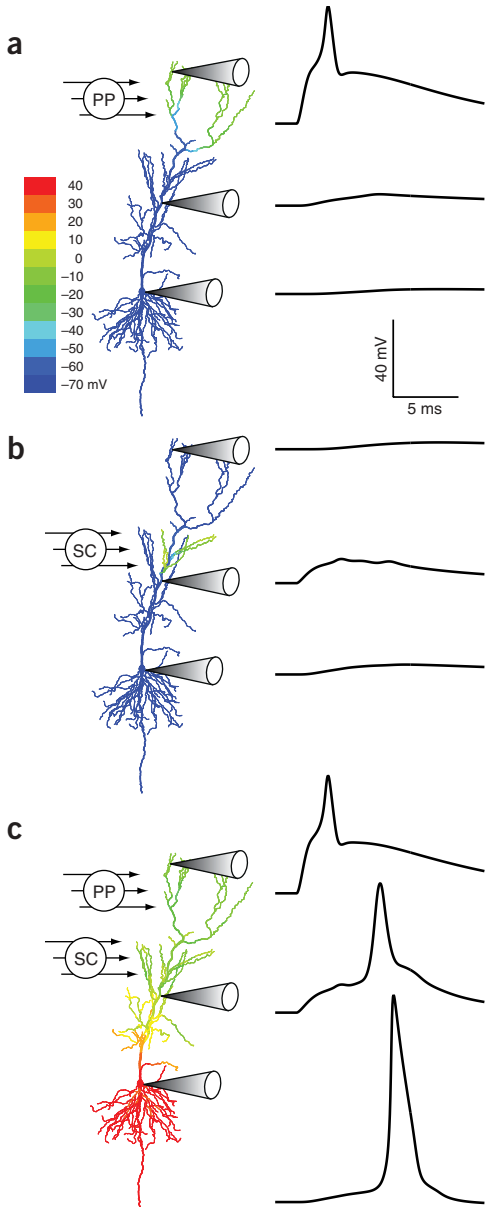

Figure 3 Gating of perforant-path–evoked dendritic spikes by Schaffer-collateral evoked EPSPs. (**a**) Color map of peak depolarization and voltage versus time plots at three dendritic locations for activation of 10% of PP synapses (one trial) in the weak dendritic excitability model. (**b**) Response of the same model to activation of 3% of SC synapses in the upper apical dendrites. (**c**) Response of the same model to coincident activation of 10% PP and 3% SC synapses. Animations of these simulations in this and the other reconstructed cell are provided in **Supplementary Videos 3–8**. Scales in **a** apply to **b** and **c** as well.

and soma (**Fig. 3**) This gating of perforant path–evoked dendritic spikes by Schaffer-collateral synaptic inputs was observed in both of the CA1 cell models (**Supplementary Figs. 2** and **3**; **Supplementary Videos 3–8** online).

One notable feature of the behavior of both the strong and the weak dendritic excitability models is that the number of perforant-path inputs necessary to trigger a dendritic spike in the tuft was actually lower than the number of Schaffer-collateral inputs necessary to trigger a dendritic spike in the upper apical dendrites. In the strong excitability model, activation of a minimum of ~2% of perforant-path inputs resulted in dendritic spikes on at least some trials, compared to at least 3% for the Schaffer-collateral input (**Fig. 2c,d**, left). About 4% of each input was necessary to produce an action potential on half of the trials (**Fig. 2b**, left), but because there were fewer synapses in the perforant-path pool (Methods), fewer perforant-path synapses were needed to produce half activation. In the weak excitability model, >3% of perforant-path synapses produced tuft spikes (**Fig. 2d**, right), compared to >5% of Schaffer-collateral synapses required to produce upper apical dendritic spikes (**Fig. 2b**, right). The lower number of perforant-path synapses required to produce dendritic spikes, in both the strong and weak excitability models, is attributable to the high input impedance of the small-diameter tuft branches.

A possible limitation of our models, which were originally designed to reproduce action potential backpropagation[14], is that they used a minimal repertoire of voltage-gated conductances. Although these models produced dendritic spikes without changes from their original forms, they are clearly very simple models. Nevertheless, the models make some interesting predictions concerning the response to distal synaptic activation. To determine if these predictions were robust, we used a more complex model, which reproduces many aspects of CA1 pyramidal neuron excitability[17]. This model contains a variety of conductances missing from our models, including H current, Ca^{2+} currents and Ca^{2+}-activated K^+ currents. Neither the presence of these additional conductances nor the longer dendrites in this model altered the basic behavior we have described. Strong activation of distal synaptic inputs triggered dendritic spikes that failed to propagate to the soma unless synapses on the apical dendrites below the tuft were also activated (**Supplementary Fig. 4** online).

A potentially important aspect of the interaction between perforant-path and Schaffer-collateral synaptic inputs is their timing. We used our models to explore the timing relationship necessary to obtain gating of forward-propagating dendritic spikes. Strong perforant-path activation (8%—sufficient to induce dendritic spikes on most trials) was simulated in the weak dendritic excitability model, and both the strength and timing of the simulated distal Schaffer-collateral input were varied. Action-potential probability was greatest when the two inputs were coincident, and the efficiency of gating decreased as the delay between the two inputs increased (**Fig. 4**). The exact nature of the interaction between the Schaffer-collateral and perforant-path inputs depended on synaptic strength and timing in a complex way. For 3.5% Schaffer-collateral activation, timing could vary by a few milliseconds, but Schaffer-collateral input preceding perforant-path input was slightly more effective than the reverse. For 5% Schaffer-collateral activation, the interaction was stronger and the range of effective timing was broader. In contrast to the weaker Schaffer-collateral stimulus, however, the 5% Schaffer-collateral input was most effective at gating the dendritic spikes if it came slightly after the perforant-path input.

Mechanism of dendritic spike gating

We explored the mechanism by which the Schaffer-collateral input facilitates the forward propagation of distally evoked dendritic spikes, by examining the voltage in the dendritic tree for Schaffer-collateral stimuli just below and just above threshold for successful propagation (**Fig. 5**). Perforant-path inputs were simulated on each apical branch and set to conductances large enough to evoke dendritic spikes in the apical tuft. A weak Schaffer-collateral input (3 nS) was too small to facilitate propagation of the dendritic spike into the main apical dendrites (**Fig. 5a–c**, left). In this case, the voltage near the main bifurcation in the apical dendrites peaked about 4 ms after the onset of

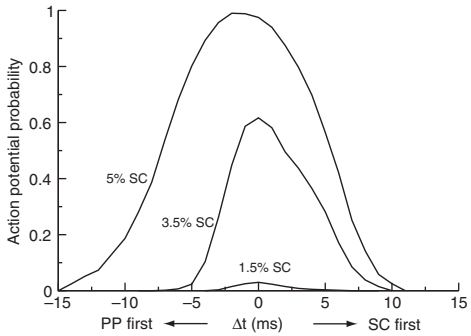

Figure 4 Dependence of PP-evoked dendritic spike propagation on the strength and timing of SC activation. Action-potential probability (soma or axon) is plotted as a function of the time difference between PP activation (8%) and SC activation (1.5, 3.5 or 5%). Probabilities were determined from 200 trials of randomly placed synapses for each value of %SC and latency (1 ms intervals).

the synaptic inputs (6.3 ms from the beginning of the simulation). A slightly larger Schaffer-collateral input (4 nS) was sufficient to successfully facilitate propagation through the main bifurcation and into the primary apical dendrite (**Fig. 5a–c**, right). In this case, the spike in the branch point occurred about 1 ms later than the peak of the failed spike in the previous case.

We found that the spike did not propagate beyond the large branch point that separates the primary apical dendrite from the apical tuft (**Fig. 5a**, left; note sharp drop in maximum voltage around 400 μm in **Fig. 5b**, left; see also **Figs. 1b** and **3**). The low safety factor for propagation of spikes through branch points is a known consequence of the decreased impedance at branch points[19,20]. In our models of CA1 neurons, reductions in spike amplitude were observed at multiple branch points, but failures of propagation were most evident at the large branch point that divided the main apical dendrite from the apical tuft. Backpropagating action potentials fail at the same location in the CA1 dendritic tree[14].

The mechanism by which Schaffer-collateral inputs rescued the propagation of dendritic spikes through this branch point can be inferred by examining the currents flowing in the major apical branch, just before the spike (4.3 ms after the onset of the synaptic stimulus). Compared to the smaller Schaffer-collateral input, which resulted in failure of the dendritic spike, the larger Schaffer-collateral synaptic input approximately tripled the Na current at this critical time and location (**Fig. 5d**). The extra Na current was the key to the successful forward propagation of the dendritic spike. A similar mechanism underlies enhancement of action-potential backpropagation by EPSPs in cortical pyramidal neurons[21].

Experimental tests of model predictions

We performed experiments to test three important predictions of the model. First, we tested the prediction that, on their own, perforant-path inputs have a limited ability to trigger action potentials in CA1 neurons. Second, we tested the prediction that when perforant-path inputs do trigger action potentials, they do so by eliciting dendritic spikes. Third, we tested the prediction that the propagation of perforant-path–evoked dendritic spikes from the apical tuft to the soma is facilitated by modest activation of Schaffer-collateral synaptic inputs.

To test whether perforant-path stimulation could trigger action potentials, we placed a large bipolar stimulating electrode in stratum lacunosum-moleculare of hippocampal slices. The perforant-path projection to CA1 is visible in this region under infrared, differential-interference contrast optics. In response to stimulation of the perforant path in the presence of GABA-receptor antagonists (Methods), we recorded monosynaptic EPSPs using whole-cell patch-clamp recordings from CA1 somata. As the stimulus intensity was increased, EPSPs increased in amplitude, but were never large enough to evoke an action potential (**Fig. 6**; average maximum EPSP = 6.7 ± 1.0 mV, $n = 11$). These results are consistent with the model's prediction that it is difficult to produce an action potential using a single stimulus of perforant path alone. In fact, it was even more difficult to get action potentials than predicted by the model, because single stimuli of the perforant path were never effective, even though some of the recorded neurons should have had relatively strong dendritic excitability[14].

To further explore the ability of perforant path to evoke action potentials, we stimulated perforant path using high-frequency bursts (100 Hz) of five or ten pulses. In most cells, it was possible to evoke action potentials using high-intensity stimulation with five pulses; moreover, in all cells, ten pulses were effective (**Fig. 6**). When spikes were driven by perforant-path synaptic stimulation in this way, action-potential threshold was lower than the threshold for evoking action potentials with current injection at the soma (**Fig. 7**). Specifically, we used somatic current injections resembling excitatory post synaptic currents (EPSCs) in the same ten-pulse pattern used for synaptic stimulation. Synaptically evoked action potentials had significantly lower thresholds than those evoked by synaptic current injection (**Fig. 7b**). In many cases, even subthreshold responses to current injection were larger than the threshold for synaptically evoked action potentials (**Fig. 7a**). These observations are consistent with the notion that perforant-path–evoked action potentials are driven by spikes that begin in the dendrites[22].

In some cases, subthreshold synaptic responses exhibited 'spikelets' (**Fig. 7c**). We have shown previously that these small spikes are the somatically recorded counterparts of large dendritic spikes[18]. Spikelets were identified more frequently during local application of tetrodotoxin (TTX) near the soma (**Fig. 7d**; Methods), suggesting that spikelets are often masked by action-potential firing. In two cells, we obtained enough trials to compare the occurrence of action potentials (control) and spikelets (local TTX) at the same perforant-path stimulus intensity; in these cells, the ratio of trials exhibiting spikelets to those exhibiting spikes was close to unity (1.04 and 0.79, 10 trials each). These results indicate that spikelets reflect dendritic spikes that have spread effectively to the soma and would usually trigger an axonal action potential.

To test whether the forward propagation of perforant-path–evoked dendritic spikes can be gated by Schaffer-collateral stimulation of the upper apical dendrites, we used a second stimulating electrode to activate Schaffer-collateral inputs (single pulse) at the end of a burst of perforant-path inputs—where the spikelets were usually observed (**Fig. 8**). Stimulation strength was set to produce single Schaffer-collateral EPSPs of 3–5 mV in the soma and single perforant-path EPSPs of 2-4 mV, which summated in bursts to 15–20 mV (at or just below threshold for spikelets). Schaffer-collateral and perforant-path responses were also simulated using EPSC-like current injections. We applied TTX near the soma so as to block action-potential firing and reveal spikelets. At the stimulus intensities used in these experiments, spikelets were never observed in response to Schaffer-collateral stimulation and were only occasionally evoked by perforant-path stimulation alone. When the two inputs were coactivated, however, the frequency of spikelets increased dramatically (**Fig. 8c**). To test whether this enhancement of spikelets was caused by summation of the somatic EPSPs, as opposed to dendritic integration of the events, we substituted a somatic, EPSC-like current injection for the Schaffer-collateral

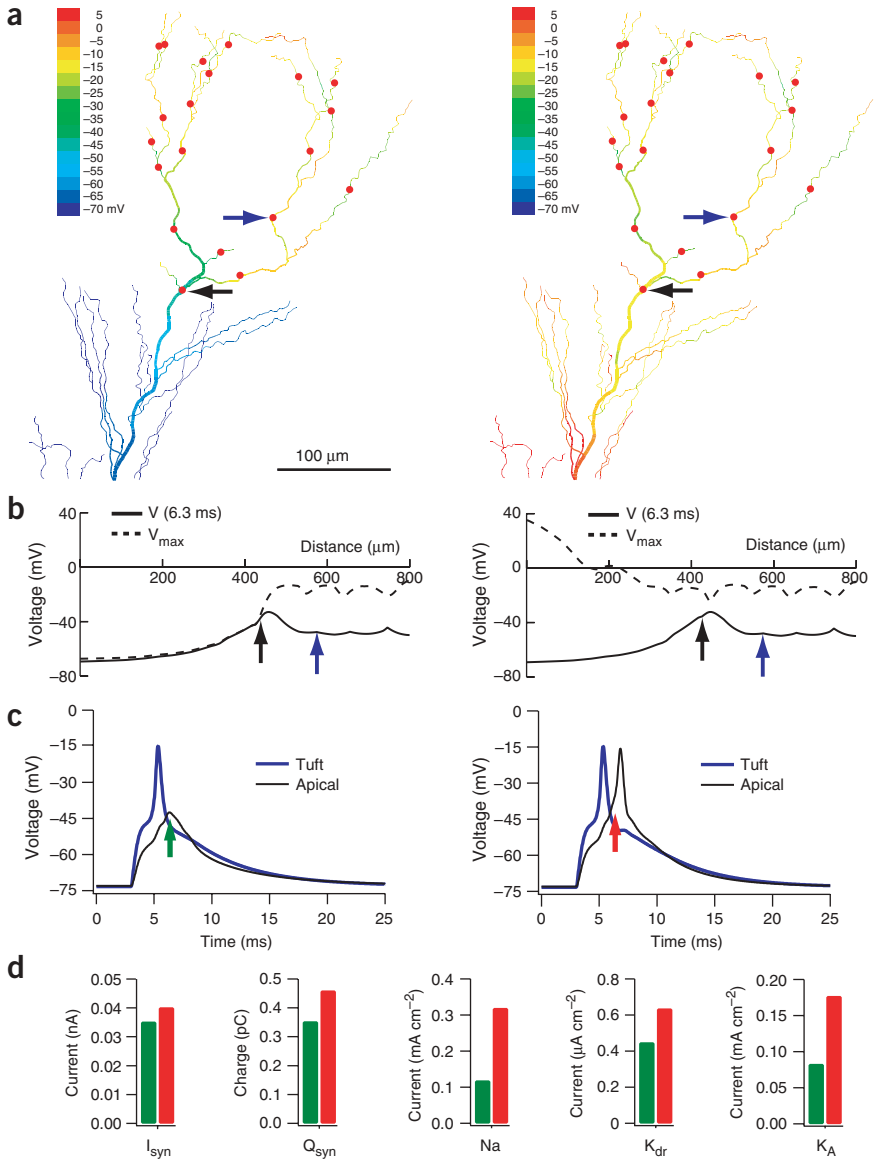

Figure 5 Mechanisms of conditional dendritic spike propagation. (**a**,**b**) Maximum voltage in upper half of the apical dendritic tree. A powerful synapse (3 nS) was placed midway along each reconstructed section of the dendritic tuft (PP, 19 synapses, red dots). A single synapse was placed near the end of the primary apical dendrite (SC, red dot with black arrow). On the left, the SC input has the same conductance as the tuft synapses and the dendritic action potentials initiated by the PP input in the tuft fail to invade the apical dendrites below the major bifurcation. On the right, the SC input has a slightly larger conductance (4 nS) and spike propagation is successful. Parameters as given in **Figure 1a**, right. (**b**) Plots showing the voltage (and maximum voltage, dashed lines) at 6.3 ms (time just before the successful dendritic spike in the main apical dendrite in **b** (right); green and red arrows in **c** along the primary apical dendrite and the tuft branch containing the synapse marked by blue arrow. Black and blue arrows correspond to locations indicated in **a**. (**c**) Voltage versus time at the tuft (blue) and apical (black) synapses. Green and red arrows indicate the apical voltage traces at 6.3 ms. (**d**) Comparison between dendritic currents at the apical synapse at 6.3 ms (time of maximum depolarization at the apical synapse for the case of propagation failure and just before the spike in the upper apical dendrite when propagation is successful). Green and red bars correspond to the points indicated by arrows in **c**. I_{syn}, instantaneous synaptic current; Q_{syn}, total synaptic charge transferred up to that time; Na, sodium current; K_{dr}, delayed rectifier potassium current; K_A, A-type potassium current.

stimulus. The amplitude of the current injection was set to yield simulated EPSPs larger than the Schaffer-collateral–evoked EPSPs (Schaffer-collateral EPSP = 4.5 ± 0.3 mV, simulated EPSP = 7.7 ± 0.8 mV, perforant-path EPSP = 3.5 ± 0.6 mV, $n = 10$). This protocol did not increase the frequency of spikelets above that observed by perforant-path stimulation alone (**Fig. 8c**), suggesting that spikelet enhancement by coincident stimulation of perforant path and Schaffer collaterals indeed reflects gating of dendritic spikes beginning in the apical tuft and propagating toward the soma.

DISCUSSION

The long distance between the perforant-path input and the axon of CA1 neurons has raised questions concerning the function of these synapses. Early reports suggested that the perforant path was mainly

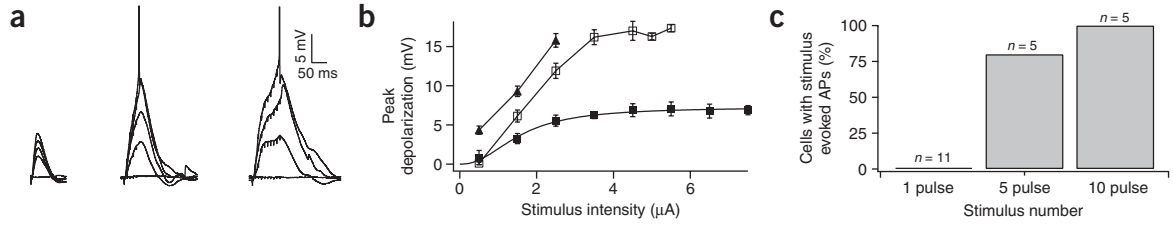

Figure 6 Experimental perforant-path stimulus-response plot. (**a**) Representative traces of EPSPs evoked by perforant path stimulation across a range of intensities. Left: EPSPs in response to a single 0.2 ms stimulus. Middle: EPSPs in response to five 0.2 ms stimuli at 100 Hz. Right: EPSPs in response to ten 0.2 ms stimuli at 100 Hz. Action potentials are truncated. (**b**) Stimulus response plot of EPSP amplitude for a representative neuron (mean ± s.e.m.; closed-squares, single stimulus; open-squares, five stimuli at 100 Hz; triangles, 10 stimuli at 100 Hz). (**c**) Summary bar graph indicating the percent of neurons in which perforant-path stimulation induced an action potential recorded at the soma in response to high-intensity stimulation.

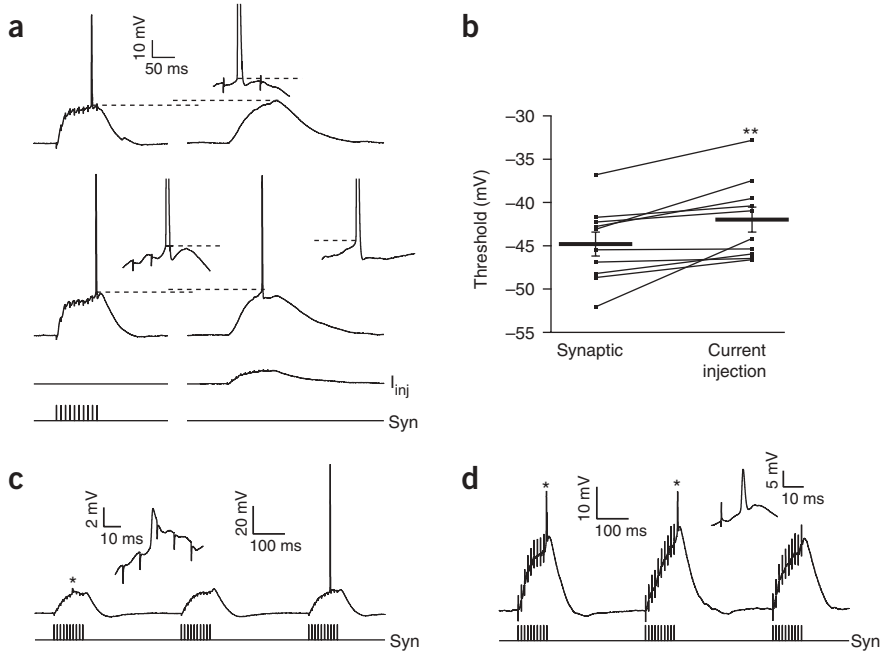

Figure 7 Dendritic spikes underlie perforant-path–evoked action potentials. (**a**) Threshold for action potentials evoked by perforant-path stimulation (Syn: 10 pulses at 100 Hz) occurs at more hyperpolarized potentials than those evoked by somatic current injection (I_{inj}). Top and bottom left: action potentials evoked by ten-pulse PP stimulation. Dashed line indicates action-potential threshold (identified as the voltage at which dV/dt first exceeds 5 mV ms^{-1}). Top right: depolarization induced by a current injection mimicking a PP-evoked EPSP burst, which failed to elicit an action potential. Dashed line indicates peak depolarization. Bottom right: current injection–evoked action potential. Dashed line indicates action-potential threshold. Insets contain magnified views of the action potentials. (**b**) Threshold of synaptically evoked action potentials is significantly hyperpolarized relative to current-injection evoked action potentials. $^{**}P < 0.05$, two-tailed Student's paired *t*-test, $n = 8$. Data from individual cells (connected points) and mean ± s.e.m. are shown. (**c**) Subthreshold spikelet (asterisk, magnified in inset) in response to minimal (sufficient to elicit a single action potential) high-frequency PP stimulation (Syn: three 10-pulse, 100-Hz bursts at 3 Hz). (**d**) Local application of TTX to the soma reveals spikelets (asterisks, second one magnified in inset) in response to high-frequency PP stimulation (Syn: three 10-pulse, 100-Hz bursts at 3 Hz).

inhibitory[5,7,23], a result of strong feedforward inhibition[5,8,9,24–28]. There is considerable evidence, however, for an excitatory influence of the perforant path on CA1 cells[5,24,27,29,30]. Furthermore, place-field firing occurs in CA1 cells deprived of Schaffer-collateral inputs by CA3 or dentate gyrus lesions[31,32]; this suggests that perforant path is capable of driving firing of CA1 neurons *in vivo*. Our findings suggest that the excitatory influence of the perforant path depends on both dendritic spikes and an interaction with Schaffer-collateral inputs.

Previous reports on the interaction between perforant-path and Schaffer-collateral inputs are seemingly contradictory. One report shows that bursts of perforant-path activation can increase the probability of Schaffer-collateral–evoked action potentials in CA1[27], whereas another study showed that perforant-path activation did not increase the response to Schaffer-collateral activation[5]. These two findings can both be understood in the context of dendritic excitability. Perforant-path stimuli that are below threshold for dendritic spikes may have little effect in the soma, because of the enormous attenuation of perforant-path EPSPs along the dendrites. Furthermore, perforant-path inputs may have a negligible effect when Schaffer-collateral inputs are strong enough to evoke spikes on their own. However, perforant-path inputs that trigger dendritic spikes on their own or in combination with milder Schaffer-collateral input can contribute to action-potential firing.

Our findings indicate that perforant-path excitatory synaptic inputs can be effective in two ways. They can reduce the number of Schaffer-collateral inputs required to trigger a dendritic spike. In this case, the Schaffer-collateral synapses are the dominant input and the perforant path can be considered modulatory. Alternatively, perforant path is the dominant input, but even a small Schaffer-collateral input can be crucial in facilitating the propagation of dendritic spikes from the apical tuft toward the soma and axon. This latter scheme indicates that perforant path can serve as the major input to CA1 neurons.

In models with strongly excitable dendrites, the perforant-path input is actually more efficacious than distal Schaffer-collateral inputs, owing to the generation of reliably propagating dendritic spikes in the small, high-impedance branches of the apical tuft. In models with weakly excitable dendrites, dendritic spikes are also readily triggered by perforant-path input, but their propagation toward the soma is unreliable. Activation of Schaffer-collateral synaptic inputs, however, promotes the forward propagation of perforant-path–evoked distal dendritic spikes. This synaptic gating of dendritic spike propagation is consistent with previous reports that dendritic spike propagation is facilitated by the depolarization of the apical dendrites[33] and resembles a similar effect predicted to occur stochastically during the background synaptic activation of CA1 dendrites[34].

In our models, the gate seems to exist near the border between perforant-path and Schaffer-collateral synaptic inputs. It exists, in large measure, because of the major bifurcation of the apical dendrites at this location in many CA1 pyramidal neurons. Both the availability of voltage-gated channels and the types of synaptic inputs will influence whether the gate is open or closed. When the gate is closed by default—as a result of a low ratio of Na^+ to K^+ channels (weak dendritic excitability[14])—it can be opened by a modest Schaffer-collateral synaptic input. Our experiments also suggest that bursts of perforant-path input could lead to successful forward propagation of dendritic spikes—an effect that can be reproduced in the models (data not shown). Thus, perforant-path inputs may open the gate on their own, without the help of Schaffer-collateral inputs. To determine whether this is likely to happen *in vivo*, it will be important for future work to determine the firing patterns of layer 3 pyramidal neurons of entorhinal cortex in awake, behaving animals. In our models, we also show that the gate can exist in an open state by default (strong dendritic excitability[14]). Whether neurons operate in a weak or strong dendritic excitability mode *in vivo* is likely to be influenced by a number of factors, including ionic conditions[33], neuromodulatory state and activity-dependent plasticity. Changes in the availability of A-type K^+ channels, which are abundant in CA1 dendrites[15], is one mechanism by which transitions between the two default states (gated closed or open) could occur[15,35,36].

Feedforward inhibition is likely to further enrich synaptic integration in distal dendrites. In the perforant path, inhibition is likely to

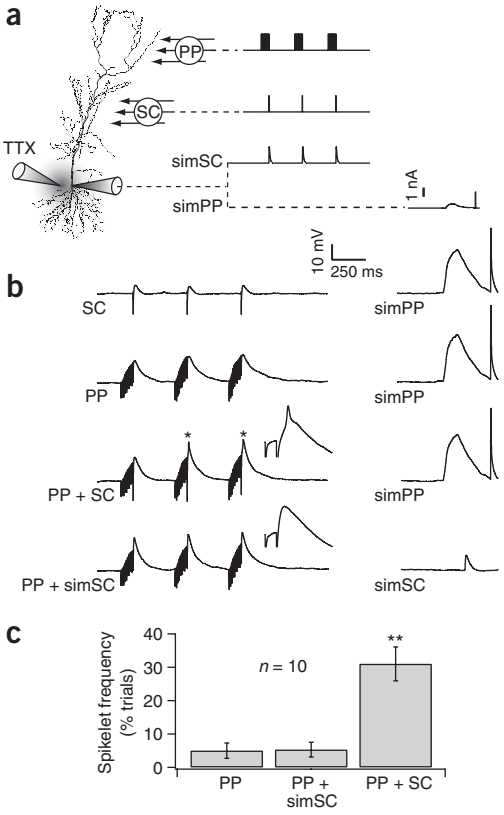

Figure 8 Coincident Schaffer-collateral stimulation increases spikelet frequency in response to perforant-path stimulation. (**a**) Experimental schematic (left): TTX was applied locally near the cell body throughout the experiment to block somatic action potentials. Stimulus protocols (right): perforant path (PP)—three 10-pulse, 100-Hz bursts at 3 Hz; Schaffer collateral (SC)—single stimuli timed to occur in coincidence with PP stimulation; simulated Schaffer collateral (simSC)—somatic current injection designed to elicit depolarizations with identical timing, similar kinetics, and equal or greater amplitude than the SC stimulation (difference of exponentials: $\tau_{rise} = 2.5$ ms, $\tau_{decay} = 10$ ms); simulated perforant-path (simPP)—somatic current injection with kinetics and amplitude similar to a single burst of PP stimulation, followed by a 2 nA, 5 ms current injection to test TTX efficacy. Action potentials were never evoked with this stimulus during TTX application, even though the stimulus was well above threshold under control conditions. (**b**) Responses to various combinations of the stimuli represented in **a**. PP + SC elicited spikelets (asterisks and inset) in a representative neuron. PP + simSC was unable to mimic the effect that SC stimulation had on PP spikelet production (inset). (**c**) Summary graph (mean ± s.e.m.) of spikelet frequency in response to PP, PP + simSC and PP + SC stimulation. $^{**}P < 0.0001$ (repeated-measures analysis of variance followed by Dunn's test with Bonferroni correction, $P < 0.01$).

temporally limit the excitatory influence of the perforant path; in contrast, in the Schaffer collaterals, inhibition may regulate the gating of distally evoked dendritic spikes. Our simulations indicate that appropriately timed Schaffer-collateral inhibition can prevent the spread of perforant-path–evoked dendritic spikes (that is, close the gate), even in strongly excitable dendrites. In weakly excitable dendrites, feedforward inhibition narrowed the time window for facilitation of dendritic spike propagation (that is, opening the gate) by the Schaffer-collateral EPSP (see **Supplementary Fig. 5** online). Modulation of inhibition is likely to be an important means of regulating synaptic integration via these mechanisms.

When TTX was locally applied near the soma, the spikelets we observed—in response to perforant-path stimulation or combined perforant-path and Schaffer-collateral stimulation—resembled the 'D-spikes' or 'fast prepotentials' observed in early intracellular recordings from hippocampal pyramidal neurons[23,37,38]. That these events are somatic indications of larger dendritic spikes is consistent with the early reports and our previous somatic and dendritic recordings[18]. More than forty years ago, it was suggested that the propagation of dendritic spikes is required for the activation of CA1 neurons by distal synaptic inputs[37]. A few years later, researchers hypothesized that the propagation of dendritic spikes might have a "low safety factor," requiring interactions at "points of confluence" in the dendrites to trigger a somatic action potential[23]. Still later, it was suggested that spikes originating in the apical tuft of neocortical pyramidal neurons could be modulated by synaptic inputs along the apical trunk[39]. Our findings validate these predictions by demonstrating such interactions in the distal dendrites of CA1 pyramidal neurons.

Whether such interactions occur in other neurons remains to be determined. In layer 5 pyramidal neurons, distal input can increase the efficacy (gain) of a more proximal input[40]. This resembles the modulatory effect we describe, but the mechanism may be different. In the neocortex, this effect occurs at least in part through the enhancement of action potential bursting, via an interaction between back-propagating action potentials and distal synaptic inputs[40,41], which has not yet been described in CA1 pyramidal neurons. The situation where the distal input can serve as the dominant input and be modulated by a modest proximal input has not been studied in cortical pyramidal neurons. Thus, it will be important for future studies to determine whether this gating of distal dendritic spikes is a general feature of pyramidal neurons in various cortical regions.

METHODS

Computational modeling. All simulations were performed using the NEURON simulation environment[42] using a 64-processor Beowulf cluster. Data presented in **Figures 1** through **4** are from one reconstructed CA1 pyramidal cell. An additional reconstructed cell was used to repeat the numerical experiments, yielding qualitatively similar results. The model cells, along with all code for our simulations, are freely available on the web (http://www.northwestern.edu/dendrite). A third reconstructed cell, using a separate model of active dendritic channels was obtained from B. Mel (Univ. Southern California, http://www-lnc.usc.edu/CA1-pyramidal-cell-model/)[17] and used to verify the results of the other cells.

Passive and active properties of the models. Our models were prepared from CA1 neurons reconstructed after staining following intracellular biocytin filling in hippocampal slices from 55–57-d-old Wistar rats. The resulting compartmental models included passive membrane properties ($R_m = 40{,}000\ \Omega cm^2$, $C_m = 0.75\ \mu F\ cm^{-2}$, $R_i = 200\ \Omega cm$) and three voltage-gated conductances: a Na^+ conductance, a delayed rectifier K^+ conductance and two variants of an A-type K^+ conductance, implemented as described[14,16]. Additional details regarding the models used here are provided in the Results section and **Figure 1**.

Synapse distribution. Synapses were distributed throughout the dendritic arbor of the reconstructed cells, with total of about 27,000 synapses in each of the first two reconstructed cells. The number and distribution of these synapses was modeled in accordance with experimental data[43]. In our study, only synapses in the distal apical dendrites were activated. Densities of excitatory synapses were higher in distal stratum radiatum (that is, distal Schaffer collaterals) than in stratum lacunosum-moleculare (that is, perforant path). The third cell was larger than the others (straight-line distance from soma to distal tip approximately 1,100 μm as opposed to 700 μm for the other two cells) and therefore included more synapses (44,391 total). As a result, lower percentages of synapses were needed to elicit dendritic spikes and somatic actions potentials in the third model.

Synapse properties. AMPA receptor–mediated synaptic conductances were modeled as the difference of two exponentials (τ_{rise} of 0.2 ms and τ_{decay} of 2.0 ms) with a reversal potential of 0 mV. The conductance of a single AMPA synapse was set to 0.18 nS, a value chosen because it produced a somatic EPSP of 0.2 mV when activated at a synapse 50 µm from the soma[44].

Schaffer-collateral and perforant-path inputs. Schaffer-collateral input was simulated as the activation of a percentage of total synapses present in the distal apical dendrites, approximately 250–500 µm from the soma. On each simulation trial, a percentage of synapses were chosen randomly from the available pool. For the first two model cells, the total number of synapses (100% activation) available for distal Schaffer-collateral input were 3,838 and 4,760. The third cell was larger and had 10,110 synapses available for distal Schaffer-collateral input. Perforant-path input was modeled as the activation of a percentage of available synapses in the apical tuft. For the first two cells, these synapses were situated approximately 500–750 µm from the soma whereas for the third cell, this distance was approximately 700–1,100 µm. As for the Schaffer-collateral input, perforant-path synapses were chosen randomly from the available pool on any individual trial. The numbers of synapses for the three cells were 2,511, 1,407 and 2,968.

Hippocampal slices preparation. All animal procedures were approved by the Northwestern University Animal Care and Use Committee. Transverse hippocampal slices were obtained from 4–5-week-old male Wistar rats. Rats were anesthetized with halothane (Sigma-Aldrich), perfused transcardially with ice-cold artificial cerebrospinal fluid (aCSF) and decapitated. The brain was then removed from the skull and transverse hippocampal slices (300 µm thick) were prepared using a vibratome. The extracellular solution used in slice preparation and incubation (20–30 min at 35 °C) was either standard aCSF (125 mM NaCl, 25 mM dextrose, 25 mM $NaHCO_3$, 2.5 mM KCl, 1.25 mM NaH_2PO_4, 2 mM $CaCl_2$ and 1 mM $MgCl_2$) or a sucrose-based solution (75 mM sucrose, 75 mM NaCl, 25 mM dextrose, 25 mM $NaHCO_3$, 7 mM $MgCl_2$, 2.5 mM KCl, 1.25 mM NaH2PO4 and 0.5 mM $CaCl_2$). All solutions were bubbled with 95% O_2 and 5% CO_2 to maintain a pH of 7.4. Following incubation, but before recording, slices were maintained at room temperature (22 °C). Three of the experiments shown in **Figure 8** were repeated in aCSF containing higher K^+ (3 mM) and lower Ca^{2+} (1.3 mM with 0.7 mM Mg^{2+}), which enhances dendritic excitability[33]. Despite this increase in dendritic excitability, the results shown in **Figure 8** were not affected by ionic conditions.

Patch-clamp recording. Individual slices were held in a small chamber perfused with aCSF at 1–3 mL min^{-1} (37 °C) and visualized with an upright, fixed-stage microscope (Zeiss Axioscop 2 FS plus) using differential interference-contrast, infrared video microscopy. Whole-cell current-clamp recordings were made with a BVC-700 amplifier (Dagan Instruments) and patch electrodes with an open tip resistance of 3–4 MΩ. Series resistance (3–25 MΩ) and capacitance were compensated using the amplifier. The intracellular solution contained 115 mM potassium gluconate, 20 mM KCl, 10 mM sodium phosphocreatine, 10 mM HEPES, 2 mM Mg-ATP, 0.3 mM Na-GTP and 0.1% biocytin. Only cells with membrane potentials less than −55 mV at the onset of the whole-cell recording were used for experiments. In most experiments, cells were maintained at −67 mV throughout the experiment with DC current injection as needed. In three of the experiments shown in **Figure 8**, however, cells were held at the resting potential (that is, no holding current); no significant differences in the results were noted.

Synaptic stimulation. Activation of the perforant path and Schaffer collaterals was obtained with two-contact cluster electrodes (CE2D55, FHC). The Schaffer-collateral stimulating electrode was placed 100 µm to the side of the cell body of the recorded neuron and approximately halfway between the cell body layer and the perforant path (visually identified by the high density of axons). The second stimulating electrode was placed in the perforant path, 200 µm lateral to the soma of the recorded neuron. Synaptic stimulation trials were repeated at intervals of 5–15 s, to minimize effects of activity-dependent plasticity. In initial experiments, to assess the localization of synaptic stimulation, before transferring a slice to the recording chamber, we made a longitudinal cut along the border between stratum radiatum and the stratum lacunosum-moleculare. In a separate experiment, to rule out the involvement of disynaptic activation, we made a cut from the CA3/CA1 border to the CA3/granule cell border, thereby removing CA3. Cuts did not influence the efficacy of synaptic stimulation and were therefore not used in subsequent experiments.

Drugs. In all experiments, 2 µM SR95531 (Sigma-Aldrich) and 3 µM CGP52432 (Tocris Bioscience) were added to the aCSF to block $GABA_A$ and $GABA_B$ receptors, respectively. In some experiments, 10 µM TTX (Sigma-Aldrich) was dissolved in aCSF and applied locally using positive pressure (0.04–0.2 psi) applied to the back of a glass pipette (tip resistance of 3–4 MΩ) positioned 10–50 µm from the soma.

Data acquisition and analysis. Data were transferred to a computer during experiments by an ITC-18 digital-analog converter (Instrutech). Igor Pro software (Wavemetrics) was used for acquisition and analysis. Electrophysiological records were filtered at 5 kHz and digitally sampled at 50–100 kHz. Statistical tests were performed using Excel software (Microsoft) or GB-STAT (Dynamic Microsystems). All results are reported as mean ± s.e.m., and significance was determined at the $P < 0.05$ level.

Note: Supplementary information is available on the Nature Neuroscience website.

ACKNOWLEDGMENTS

We thank members of the Spruston and Kath labs and B. Mel for discussions. This work was supported by the US National Institutes of Health (NS-35180 to N.S., NS-46064 to N.S. and W.L.K., and NS-045437 to T.J.) and by the National Science Foundation (DGE-9987577 to A.R.).

COMPETING INTERESTS STATEMENT

The authors declare that they have no competing financial interests.

Published online at http://www.nature.com/natureneuroscience/
Reprints and permissions information is available online at http://npg.nature.com/reprintsandpermissions/

1. Stuart, G., Spruston, N., Sakmann, B. & Häusser, M. Action potential initiation and backpropagation in neurons of the mammalian CNS. *Trends Neurosci.* **20**, 125–131 (1997).
2. Johnston, D., Magee, J.C., Colbert, C.M. & Christie, B.R. Active properties of neuronal dendrites. *Annu. Rev. Neurosci.* **19**, 165–186 (1996).
3. Häusser, M., Spruston, N. & Stuart, G.J. Diversity and dynamics of dendritic signaling. *Science* **290**, 739–744 (2000).
4. Amaral, D.G. Emerging principles of intrinsic hippocampal organization. *Curr. Opin. Neurobiol.* **3**, 225–229 (1993).
5. Colbert, C.M. & Levy, W.B. Electrophysiological and pharmacological characterization of perforant path synapses in CA1: mediation by glutamate receptors. *J. Neurophysiol.* **68**, 1–8 (1992).
6. Desmond, N.L., Scott, C.A., Jane, J.A., Jr. & Levy, W.B. Ultrastructural identification of entorhinal cortical synapses in CA1 stratum lacunosum-moleculare of the rat. *Hippocampus* **4**, 594–600 (1994).
7. Levy, W.B., Colbert, C.M. & Desmond, N.L. Another network model bites the dust: entorhinal inputs are no more than weakly excitatory in the hippocampal CA1 region. *Hippocampus* **5**, 137–140 (1995).
8. Soltesz, I. Brief history of cortico-hippocampal time with a special reference to the direct entorhinal input to CA1. *Hippocampus* **5**, 120–124 (1995).
9. Yeckel, M.F. & Berger, T.W. Monosynaptic excitation of hippocampal CA1 pyramidal cells by afferents from the entorhinal cortex. *Hippocampus* **5**, 108–114 (1995).
10. Golding, N.L. & Spruston, N. Dendritic sodium spikes are variable triggers of axonal action potentials in hippocampal CA1 pyramidal neurons. *Neuron* **21**, 1189–1200 (1998).
11. Kamondi, A., Acsady, L. & Buzsaki, G. Dendritic spikes are enhanced by cooperative network activity in the intact hippocampus. *J. Neurosci.* **18**, 3919–3928 (1998).
12. Colbert, C.M. & Johnston, D. Axonal action-potential initiation and Na^+ channel densities in the soma and axon initial segment of subicular pyramidal neurons. *J. Neurosci.* **16**, 6676–6686 (1996).
13. Spruston, N., Schiller, Y., Stuart, G. & Sakmann, B. Activity-dependent action potential invasion and calcium influx into hippocampal CA1 dendrites. *Science* **268**, 297–300 (1995).
14. Golding, N.L., Kath, W.L. & Spruston, N. Dichotomy of action-potential backpropagation in CA1 pyramidal neuron dendrites. *J. Neurophysiol.* **86**, 2998–3010 (2001).
15. Hoffman, D.A., Magee, J.C., Colbert, C.M. & Johnston, D.K. K^+ channel regulation of signal propagation in dendrites of hippocampal pyramidal neurons. *Nature* **387**, 869–875 (1997).
16. Migliore, M., Hoffman, D.A., Magee, J.C. & Johnston, D. Role of an A-type K^+ conductance in the back-propagation of action potentials in the dendrites of hippocampal pyramidal neurons. *J. Comput. Neurosci.* **7**, 5–15 (1999).
17. Poirazi, P., Brannon, T. & Mel, B.W. Arithmetic of subthreshold synaptic summation in a model CA1 pyramidal cell. *Neuron* **37**, 977–987 (2003).

18. Golding, N.L., Staff, N.P. & Spruston, N. Dendritic spikes as a mechanism for cooperative long-term potentiation. *Nature* **418**, 326–331 (2002).
19. Goldstein, S.S. & Rall, W. Changes of action potential shape and velocity for changing core conductor geometry. *Biophys. J.* **14**, 731–757 (1974).
20. Manor, Y., Koch, C. & Segev, I. Effect of geometrical irregularities on propagation delay in axonal trees. *Biophys. J.* **60**, 1424–1437 (1991).
21. Stuart, G.J. & Hausser, M. Dendritic coincidence detection of EPSPs and action potentials. *Nat. Neurosci.* **4**, 63–71 (2001).
22. Anderson, P., Storm, J. & Wheal, H.V. Thresholds of action potentials evoked by synapses on the dendrites of pyramidal cells in the rat hippocampus *in vitro*. *J. Physiol. (Lond.)* **383**, 509–526 (1987).
23. Andersen, P. & Lomo, T. Mode of activation of hippocampal pyramidal cells by excitatory synapses on dendrites. *Exp. Brain Res.* **2**, 247–260 (1966).
24. Buzsaki, G., Penttonen, M., Bragin, A., Nadasdy, Z. & Chrobak, J.J. Possible physiological role of the perforant path-CA1 projection. *Hippocampus* **5**, 141–146 (1995).
25. Empson, R.M. & Heinemann, U. The perforant path projection to hippocampal area CA1 in the rat hippocampal-entorhinal cortex combined slice. *J. Physiol. (Lond.)* **484**, 707–720 (1995).
26. Empson, R.M. & Heinemann, U. Perforant path connections to area CA1 are predominantly inhibitory in the rat hippocampal-entorhinal cortex combined slice preparation. *Hippocampus* **5**, 104–107 (1995).
27. Remondes, M. & Schuman, E.M. Direct cortical input modulates plasticity and spiking in CA1 pyramidal neurons. *Nature* **416**, 736–740 (2002).
28. Pare, D. & Llinas, R. Intracellular study of direct entorhinal inputs to field CA1 in the isolated guinea pig brain *in vitro*. *Hippocampus* **5**, 115–119 (1995).
29. Doller, H.J. & Weight, F.F. Perforant pathway activation of hippocampal CA1 stratum pyramidale neurons: electrophysiological evidence for a direct pathway. *Brain Res.* **237**, 1–13 (1982).
30. Yeckel, M.F. & Berger, T.W. Feedforward excitation of the hippocampus by afferents from the entorhinal cortex: redefinition of the role of the trisynaptic pathway. *Proc. Natl. Acad. Sci. USA* **87**, 5832–5836 (1990).
31. Brun, V.H. *et al.* Place cells and place recognition maintained by direct entorhinal-hippocampal circuitry. *Science* **296**, 2243–2246 (2002).
32. McNaughton, B.L., Barnes, C.A., Meltzer, J. & Sutherland, R.J. Hippocampal granule cells are necessary for normal spatial learning but not for spatially-selective pyramidal cell discharge. *Exp. Brain Res.* **76**, 485–496 (1989).
33. Gasparini, S., Migliore, M. & Magee, J.C. On the initiation and propagation of dendritic spikes in CA1 pyramidal neurons. *J. Neurosci.* **24**, 11046–11056 (2004).
34. Fellous, J.M., Rudolph, M., Destexhe, A. & Sejnowski, T.J. Synaptic background noise controls the input/output characteristics of single cells in an *in vitro* model of *in vivo* activity. *Neuroscience* **122**, 811–829 (2003).
35. Frick, A., Magee, J. & Johnston, D. LTP is accompanied by an enhanced local excitability of pyramidal neuron dendrites. *Nat. Neurosci.* **7**, 126–135 (2004).
36. Johnston, D., Hoffman, D.A., Colbert, C.M. & Magee, J.C. Regulation of back-propagating action potentials in hippocampal neurons. *Curr. Opin. Neurobiol.* **9**, 288–292 (1999).
37. Spencer, W.A. & Kandel, E.R. Electrophysiology of hippocampal neurons. IV. Fast prepotentials. *J. Neurophysiol.* **24**, 272–285 (1961).
38. Wong, R.K. & Stewart, M. Different firing patterns generated in dendrites and somata of CA1 pyramidal neurones in guinea-pig hippocampus. *J. Physiol. (Lond.)* **457**, 675–687 (1992).
39. Cauller, L.J. & Connors, B.W. Functions of very distal dendrites: experimental and computational studies of layer I inputs to layer V pyramidal neurons in neocortex. in *Single Neuron Computation* (eds. McKenna, T., Davis, J. & Zornetzer, S.F.) 199–230 (Academic Press, San Diego, 1992).
40. Larkum, M.E., Senn, W. & Luscher, H.R. Top-down dendritic input increases the gain of layer 5 pyramidal neurons. *Cereb. Cortex* **14**, 1059–1070 (2004).
41. Larkum, M.E., Zhu, J.J. & Sakmann, B. A new cellular mechanism for coupling inputs arriving at different cortical layers. *Nature* **398**, 338–341 (1999).
42. Hines, M.L. & Carnevale, N.T. The NEURON simulation environment. *Neural Comput.* **9**, 1179–1209 (1997).
43. Megias, M., Emri, Z., Freund, T.F. & Gulyas, A.I. Total number and distribution of inhibitory and excitatory synapses on hippocampal CA1 pyramidal cells. *Neuroscience* **102**, 527–540 (2001).
44. Magee, J.C. & Cook, E.P. Somatic EPSP amplitude is independent of synapse location in hippocampal pyramidal neurons. *Nat. Neurosci.* **3**, 895–903 (2000).